Journal of Chromatography, 606 (1992) 103–111
Elsevier Science Publishers B.V., Amsterdam

CHROM. 24 263

Unsteady heat transfer in capillary zone electrophoresis

II. Computer simulations

Michael S. Bello* and Pier Giorgio Righetti

Department of Biomedical Sciences and Technologies, University of Milan, Via Celoria 2, Milan 20133 (Italy)

(First received January 7th, 1992; revised manuscript received April 13th, 1992)

ABSTRACT

Unsteady heat transfer in capillary zone electrophoresis in considered. Equations are derived that allow the calculation of the temperature evolution of the buffer under three different modes of electrophoresis: current-, voltage- or power-stabilized. In the power-stabilized mode, the temperature increase is intermediate between those in the current- (lowest) and voltage-stabilized (highest) modes. As the shortest transient time and the smallest temperature rise correspond to the current-stabilized mode of operation, this regime is recommended for temperature-sensitive separations and evaluations of the capillary heat-transfer coefficient, especially in the case of instrumentation-lacking forced cooling.

INTRODUCTION

Any electrophoresis process, whenever it occurs, is accompanied by internal heat generation caused by a dissipation of energy of moving ions. Heat exchange of the electrolyte solution with the outer medium is possible only through the surface of the electrophoresis cell. This inevitably leads to the appearance of temperature gradients within the solution and to a rise in the average temperature of the buffer. Changes in the buffer temperature affect its conductivity, dissociation constants (pK and hence pH), the wall ζ-potential and the mobilities of the separated particles and, as a result, influence the electrophoretic separation.

Correspondence to: Professor Pier Giorgio Righetti, Department of Biomedical Sciences and Technologies, University of Milan, Via Celoria 2, Milan 20133, Italy.

* Permanent address: Institute of Macromolecular Compounds, Academy of Sciences, Bolshoi pr. 31, St. Petersburg 199004, Russia.

The importance of the heat-transfer process in capillary electrophoresis was realized a long time ago. However, systematic theoretical and experimental studies of temperature fields in the capillary, conditions of cooling and the like have been published only recently [1–7].

Experimental investigations have shown a nonlinear dependence of the electric current on the applied voltage [1–3], high sensitivity of the electric current to variations of cooling conditions [1] and a decrease in the theoretical plate height due to inadequate cooling [1]. The advantages of forced or Peltier cooling have been demonstrated by Nelson *et al.* [1]. It has also been reported that at high currents the electrophoresis process becomes unstable [1].

Theoretixcal papers mostly deal with the radial temperature distribution within the capillary. Gobie and Ivory [2] unambiguously explained the deviations from Ohm's law by the temperature dependence of the conductivity. They considered the steady-state temperature distribution within the capillary by taking into account the temperature

0021-9673/92/$05.00

dependence of the buffer conductivity[a]. They predicted and experimentally verified a situation in which the temperature increases infinitely. For this case they introduced the term "autothermal runaway". We accept this term and will use it below, but the mathematical treatment in ref. 2 and the equations therein do not consider time-dependent processes.

The aim of this study was to consider the transient process of establishing the steady-state temperature distribution. The following arguments justifying the significance of this problem can be provided: (1) such an unsteady process exists, it has been observed experimentally [1] and, therefore, it should be studied; (2) the heat transfer during electrophoresis under stacking conditions [6], when the electric conductivity of the sample zone differs from that of the buffer is, in fact, an unsteady process; and (3) it can be assumed that the process of micelle formation in micellar electrokinetic chromatography [8] depends not only on the resulting temperature but also on the transient temperature regime.

Below we formulate equations of unsteady heat transfer in the capillary. The approximate solution of these equations allows us to calculate a time dependence of the electric current in the capillary after a voltage has been applied for different operating modes from a power supply (voltage-, current- or power-stabilized mode). A transient time (*i.e.*, the time necessary to achieve a steady state) is calculated as a function of the capillary parameters and also parameters of the electrophoretic process.

THEORY

This part presents the general equations of unsteady heat transfer and boundary conditions in both dimensional and dimensionless forms and sets the problem in mathematical terms.

We consider the same system dealt with by others [2,6], consisting of a lumen, a fused-silica wall and a polyimide coat (Fig. 1). The electric conductivity of the buffer is assumed to be linearly dependent on temperature [2]. The difference between previous studies and this work is that we consider the development of the temperature field not only in space but also in time. The behaviour of the temperature field in the lumen, in the wall and in the coat is governed by the equations of unsteady heat transfer[b] [9]:

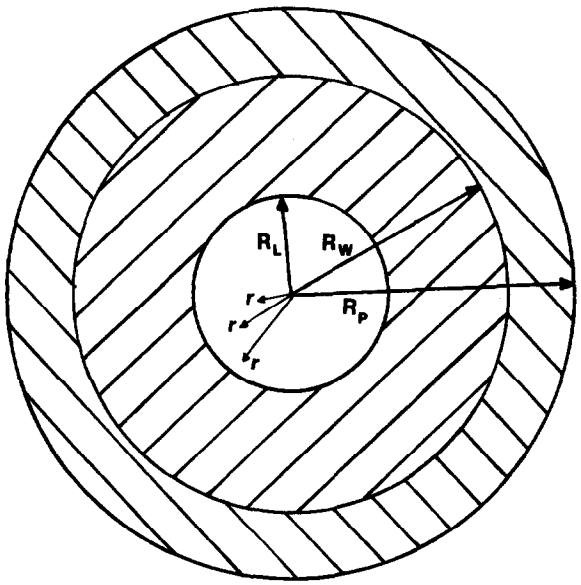

Fig. 1. Schematic representation of the capillary cross-section. R_L, R_W and R_P = radii of the lumen, wall and polyimide coat, respectively; r = distance between the centre of the capillary and any point of the cross-section (modified from Gobie and Ivory [2]).

$$\rho_L C_{pL} \cdot \frac{\partial T}{\partial t} = \chi_L \cdot \frac{1}{r} \cdot \frac{\partial}{\partial r}\left(r \cdot \frac{\partial T}{\partial r}\right) + q \quad 0 \leqslant r < R_L \quad (1)$$

$$\rho_W C_{pW} \cdot \frac{\partial T}{\partial t} = \chi_W \cdot \frac{1}{r} \cdot \frac{\partial}{\partial r}\left(r \cdot \frac{\partial T}{\partial r}\right) \quad R_L \leqslant r < R_W \quad (2)$$

$$\rho_P C_{pP} \cdot \frac{\partial T}{\partial t} = \chi_P \cdot \frac{1}{r} \cdot \frac{\partial}{\partial r}\left(r \cdot \frac{\partial T}{\partial r}\right) \quad R_W \leqslant r < R_P \quad (3)$$

where T is the temperature, t the time, r the radius, ρ_L, ρ_W and ρ_P are the densities of the buffer, wall and the polyimide, respectively, C_L, C_W and C_P are their specific heat capacities, χ_L, χ_W and χ_P are their thermal conductivities, R_L, R_W and R_P are the radii of the lumen, wall and the polyimide coat, respec-

[a] A heat-transfer process is called "steady" if the temperature field does not vary with time, otherwise it is called "unsteady". These terms are used in order to avoid using "equilibrium" and "non-equilibrium", because a process of heat transfer is non-equilibrium in its nature.

[b] For symbols, see Part I [11].

tively, and q is the Joule heat generation (quantity of energy dissipated in unit volume per unit time).

The boundary conditions for eqns. 1–3 specify the finiteness of the temperature at the origin $r = 0$, the continuity of the temperature and the heat flux at the lumen–wall and wall–coat interfaces and the heat balance at the external surface of the capillary. These boundary conditions are expressed as follows:

$$T = \text{finite at } r = 0 \tag{4a}$$

$$T^- = T^+,\ \chi_L \cdot \frac{\partial T}{\partial r} = \chi_W \cdot \frac{\partial T^+}{\partial r} \text{ at } r = R_L \tag{4b}$$

$$T^- = T^+,\ \chi_W \cdot \frac{\partial T^-}{\partial r} = \chi_P \cdot \frac{\partial T^+}{\partial r} \text{ at } r = R_W \tag{4c}$$

$$-\chi_P \cdot \frac{\partial T}{\partial r} = h(T - T_C) \text{ at } r = R_P \tag{4d}$$

where the superscripts $^-$ and $^+$ indicate left and right values of the temperature and its derivative with respect to a boundary, h is the coefficient of the external heat transfer and T_C is the temperature of the coolant.

The heat-transfer coefficient depends on cooling conditions and for the case of forced cooling can be represented as follows:

$$h = Nu\chi_C/(2R_P) \tag{4e}$$

where χ_C is the thermal conductivity of the coolant and Nu is the Nusselt number, which is given by

$$Nu = 0.76Re^{0.4}Pr^{0.37} \tag{4f}$$

for the case of forced cooling and by

$$Nu = \left\{0.6 + \frac{0.387Ra^{1/6}}{[1 + (0.559/Pr)^{9/16}]^{8/27}}\right\}^2 \tag{4g}$$

for the case of lack of forced cooling [10], Re, Pr and Ra are the Reynolds, Prandtl and Rayleigh numbers, respectively, whose definition can be found also in ref. 8.

The initial condition for eqns. 1–3 is set in the following form:

$$T(r, t = 0) = T_C \tag{5}$$

An explicit expression for q appearing on the right-hand side of eqn. 1 depends on the mode in which the power supply is used. We shall distinguish three modes by which Joule heat is produced, outlined below.

Voltage-stabilized mode (E = constant)

$$q = \sigma E^2 = q_0[1 + \alpha(T - T_0)] \tag{6a}$$

$$\sigma = \sigma_0[1 + \alpha(T - T_0)] \tag{6b}$$

where σ is the electric conductivity of the buffer at temperature T, σ_0 the electric conductivity of the buffer measured at temperature T_0, α the temperature coefficient of the electric conductivity, E the electric field strength and q_0 the initial dissipated power per unit volume. In this mode the power and the electric current are time dependent.

Current-stabilized mode (I = constant)

By introducing the average electric conductivity as

$$\bar{\sigma} = 2\pi \int_0^{R_L} r\,\sigma dr/S \tag{6c}$$

where $S = \pi R_L^2$ is the area of the lumen cross-section, one obtains for E and q the following equations:

$$E = I_0/(S\bar{\sigma}) \tag{6d}$$

$$q = \sigma[I_0/(S\bar{\sigma})]^2 = q_0\sigma_0^2[1 + \alpha(T - T_0)]/\bar{\sigma}^2 \tag{6e}$$

where I_0 is the value of the current which is maintained stable. It was taken into account, when deriving eqns. 6d and e, that the electric field strength may vary with time but not in radius. In the current-stabilized mode the power and the electric field (voltage) are time dependent.

Power-stabilized mode (Q = constant)

In analogy with the previous case, one obtains for q

$$q = q_0\sigma/\bar{\sigma} \tag{6f}$$

In this mode the electric field and the electric current are time dependent. In all instances we neglected the transient times of the power supply.

It is useful for further analysis to introduce several dimensionless variables. We shall use the lumen radius R_L as a length scale, the characteristic temperature difference:

$$\Delta T_{ref} = q_0R_L^2/\chi_L \tag{7a}$$

as the temperature scale and the characteristic time of thermal diffusivity:

$$\tau_c = R_L^2 \cdot \frac{\rho_L C_{pL}}{\chi_L} \quad (7b)$$

as the time scale.

The autothermal parameter k^2 is defined as follows:

$$k^2 = \alpha \Delta T_{ref} \quad (7c)$$

the dimensionless temperatures are

$$\vartheta = (T - T_0)/\Delta T_{ref},\ \vartheta_C = (T_C - T_0)/\Delta T_{ref} \quad (7d)$$

and the Biot number is defined by

$$Bi = hR_L/\chi_L \quad (7e)$$

The average dimensionless temperature $\bar{\vartheta}$ is given by

$$\bar{\vartheta} = \frac{2}{R_L^2} \int_0^{R_L} \vartheta r dr \quad (8)$$

Eqns. 1–6 form a set of non-linear integro-differential equations of conjugated heat transfer. In the particular case of the voltage-stabilized mode of operation, this system becomes linear and merely differential. This case is the most common in capillary electrophoresis practice and will be studied in detail below. However, we shall consider in a simplified form all modes of operation listed above.

APPROXIMATE ANALYSIS OF THE UNSTEADY HEAT TRANSFER

In this part we shall use approximate solutions for the buffer average temperature for different modes of power supply (see also Part I [11]). Although not quantitative, such results are useful for a better understanding of the physical nature of the unsteady process.

The approximate solution for the average buffer temperature in the case of good cooling conditions (see Part I [11]) is given by

$$\bar{\vartheta}_a = \bar{\vartheta}_{a_s} + [\vartheta_C - \bar{\vartheta}_{a_s}] \exp(-t/\tau) \quad (9)$$

$$\bar{\vartheta}_{a_s} = \frac{2Bi_{0A}\vartheta_C + 1}{2Bi_{0A} - fk^2} \quad (9a)$$

$$\tau = (2Bi_{0A} - fk^2)^{-1} \quad (9b)$$

where the factor f is

$$f = \begin{cases} 1 \text{ for the voltage-stabilized mode} \\ -1 \text{ for the current-stabilized mode} \\ 0 \text{ for the power-stabilized mode,} \end{cases}$$

$\bar{\vartheta}_a$ is the approximate average temperature, Bi_{0A} is the overall Biot number defined below, $\bar{\vartheta}_{a_s}$ is the steady-state (*i.e.*, independent of time) part of the solution and τ is the characteristic time of the transient process.

The overall Biot number used by Gobie and Ivory [2] in our notation has the following form:

$$Bi_{0A} = \beta_{WL}\left\{\ln(R_W/R_L) + \frac{1}{\beta_{PW}}\left[\ln(R_P/R_W) + \frac{R_L\beta_{PL}}{R_P Bi}\right]\right\}^{-1} \quad (10)$$

The solution, as seen from eqn. 9, consists of two parts, one of which is the steady-state temperature and the other is the transient part vanishing in time. During a period of time equal to τ, the unsteady part of the temperature decreases e times. We shall define the transient time of the process τ_{tr} as the time necessary for decrease in the unsteady part of e^4 times ($1/e^4 = 1.8\%$):

$$\tau_{tr} = 4\tau \quad (9c)$$

The dependences of the dimensionless average temperature $\bar{\vartheta}_a$ on the dimensionless time calculated using eqns. 9 for three modes of operation are shown in Fig. 2. The curves corresponding to different

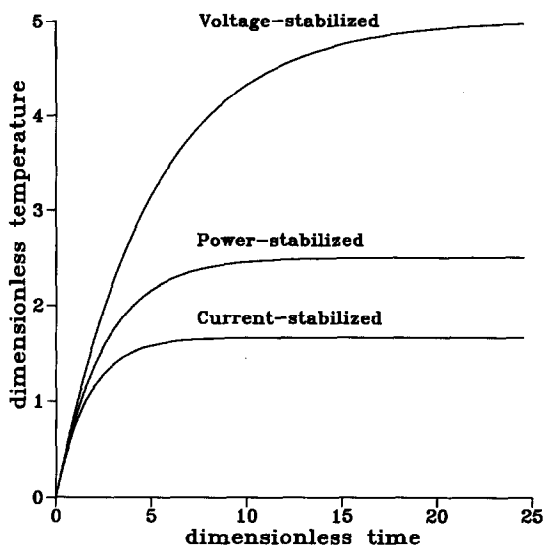

Fig. 2. Dimensionless temperature as a function of dimensionless time (approximate equations) for three possible modes of power supply operation. $Bi_{0A} = 0.2$, $k^2 = 0.2$. Note how the current-stabilized mode corresponds at any given time to the lowest temperature evolution.

modes of operation are calculated for $Bi_{0A} = 0.2$ and $k^2 = 0.2$. It is seen from Fig. 2 that the shortest transient time and the smallest temperature increase correspond to the current-stabilized mode. The longest transient time and the largest temperature increase correspond to the voltage-stabilized mode, while the power-stabilization mode lies in the middle. The difference between these three modes is caused by the temperature dependence of the buffer velocity.

Of course, these effects are pronounced only for the case of relatively small Biot numbers Bi_{0A} (poor cooling conditions) and relatively large values of the autothermal parameter k^2 (high voltage, large diameter of capillary, high buffer conductivity), or, better, for the case when the Biot number and the autothermal parameter are of the same order of magnitude. Thus, if $k = 0$, the values for τ and $\bar{\vartheta}_{a_s}$ (see eqns. 9) will be the same for all three cases. It is also seen from eqns. 9 that the transient time τ and the average buffer temperature for the voltage-stabilized mode increase infinitely if k^2 approaches $2Bi_{0A}$. This result is in agreement with the study of Gobie and Ivory [2], who called this phenomenon the "autothermal runaway". It is interesting that neither τ nor $\bar{\vartheta}_{a_s}$ is affected by the autothermal parameter k^2 in the power stabilization mode. It should be stressed that this approximate theory is limited to the case of a capillary with a relatively thin wall and coating.

UNSTEADY HEAT TRANSFER IN A POWER-STABILIZED MODE

This part aims at presenting results of mathematical modelling of the transient heat transfer in the power-stabilized mode governed by eqns. 1–6. In order to calculate temperature profiles across the capillary and transient times, we used the procedure described in Part I [11].

As the temperature regime depends significantly on the capillary dimensions and on the cooling conditions, we shall distinguish three types of capillaries and three modes of cooling.

The capillary types are thin, with I.D. < 50 μm, intermediate, with 50 μm $<$ I.D. < 150 μm, and thick, with I.D. > 150 μm. The thermal properties of the fused-silica wall and polyimide coating were taken from the Standard Product List of Polymicro Technologies (Phoenix, AZ, USA). The thermal properties of the buffer are assumed to be identical with those of water and the electrical conductivity of the buffer and its thermal coefficient were taken from ref. 2. All data used are presented in Table I.

As representative examples of thin, intermediate and thick capillaries we chose those with I.D. = 50 μm, O.D. = 363 μm for thin, I.D. = 150 μm, O.D. = 363 μm for intermediate and I.D. = 530 μm, O.D. = 700 μm for thick. The thickness of the polyimide coating was assumed to be 15 μm in all instances.

The three modes of cooling we distinguish are lack of forced cooling, forced air cooling and forced liquid cooling.

The heat-transfer coefficient for the case of lack of forced cooling was evaluated by using eqns. 4e and g with parameters corresponding to dry air at 25°C and the characteristic temperature difference (for evaluation of the Rayleigh number) equal to 30°C.

The values of heat-transfer coefficients in air and liquid cooling systems used in the Beckman apparatus for the capillary with $R_P = 165$ μm are $h_{air} = 239.54$ W/m^2 · K for the air cooling system and $h_{liq} = 1136$ W/m^2 · K for the liquid cooling system (data kindly provided by Dr. K. Anderson, Beckman Instruments, Palo Alto, CA, USA). We recalculate the heat transfer coefficients by multiplying these values by the factor $(R_P/165)^{-0.6}$, according to eqns. 4f and e.

The evolution of temperature profiles across the

TABLE I

PHYSICAL PARAMETERS USED FOR COMPUTER SIMULATIONS

Parameter	Value	Parameter	Value
ρ_L[a]	1 g/cm^3	χ_L[c]	0.61 W/mK
ρ_W	2.15 g/cm^3	χ_W	1.5 W/mK
ρ_P	1.42 g/cm^3	χ_P	0.15 W/mK
C_{PL}[b]	4.18 J/g	σ_0[d]	7.5 mS/cm
C_{PW}	1 J/g	α[e]	$2.17 \cdot 10^{-2}$ K^{-1}
C_{pP}	1.1 J/g		

[a] Density.
[b] Specific heat capacity.
[c] Thermal conductivity.
[d] Electric conductivity of the buffer.
[e] Thermal coefficient of electric conductivity.

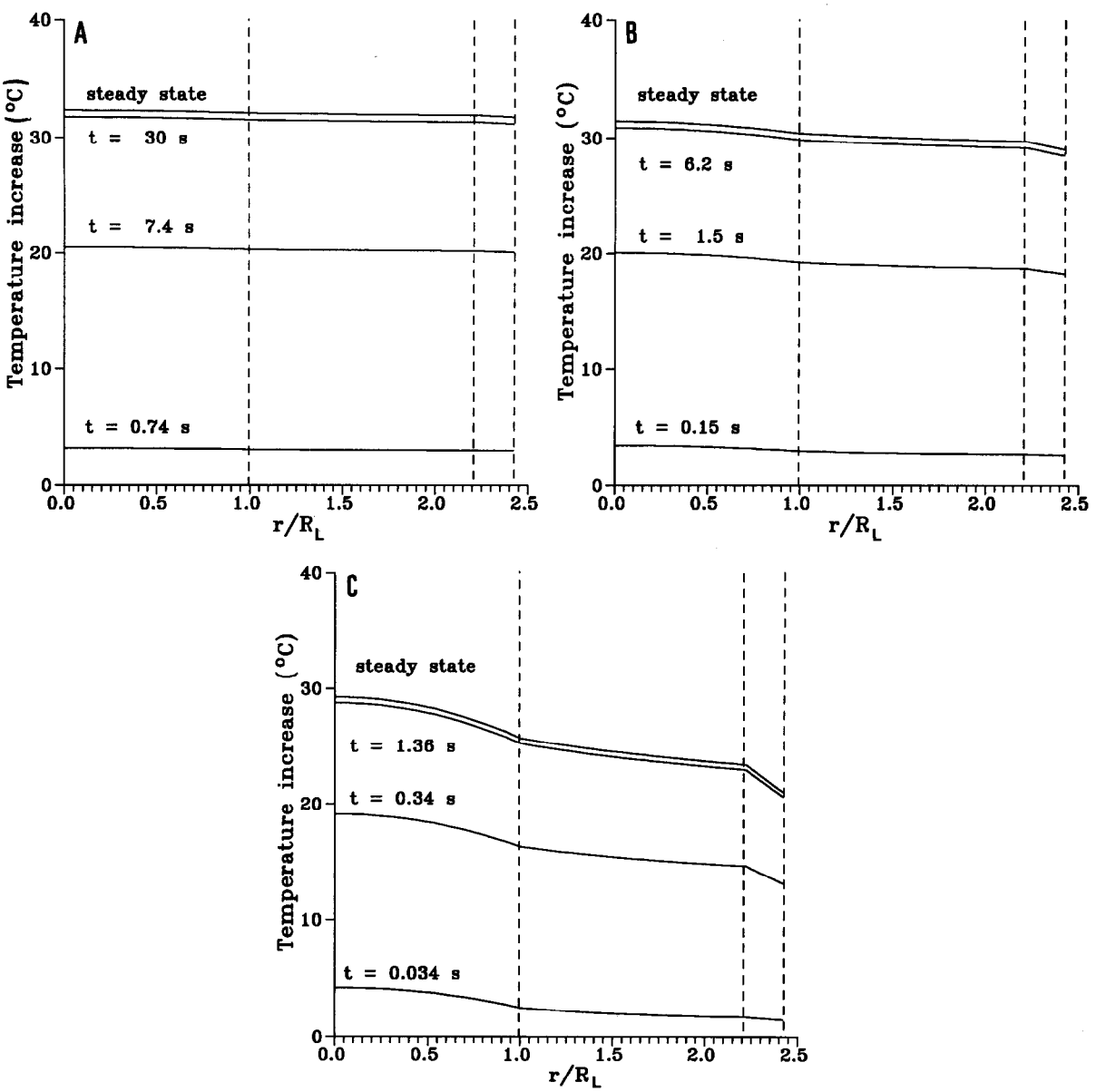

Fig. 3. Temperature profiles across the capillary at different times as a function of the r/R_L ratio (where r = distance between any point in the section of Fig. 1, up to RP, and the centre of the capillary; R_L = radius of the lumen of the capillary). In all three simulations, the lower three curves represent time points equal to 0.1τ, τ and 4τ. The upper curve in all figures corresponds to the steady-state temperature distribution. (A) Lack of forced cooling, voltage gradient 90 V/cm; (B) air-cooling, voltage gradient 190 V/cm; (C) liquid cooling, voltage gradient 360 V/cm. Note that, in all simulations, the value of zero on the abscissa represents the centre of the lumen of the capillary; therefore, a full representation of the temperature profile in the entire capillary should correspond to a specular doubling of the image on the left-hand side of each figure. The vertical dashed lines represent at $x = 1$, end of the lumen; at $x = 2.22$, end of the wall; and at $x = 2.42$, end of the polyimide coat of the capillary.

TABLE II

TRANSIENT TIME AS A FUNCTION OF COOLING MODE AND CAPILLARY SIZE (CALCULATED AT $\Delta T \approx 30°C$)

Type of capillary	Parameter	Type of cooling		
		None	Air cooling	Liquid cooling
Thin (I.D. = 50 μm, O.D. = 363 μm)	E (V/cm)	250	550	1050
	τ_{tr} (s)	25	5.2	1.2
Intermediate (I.D. = 150 μm, O.D. = 363 μm)	E (V/cm)	90	190	360
	τ_{tr} (s)	29.6	6.2	1.4
Thick (I.D. = 530 μm, O.D. = 700 μm)	E (V/cm)	28	65	125
	τ_{tr} (s)	120	21	4.8

capillary of the intermediate type for three modes of cooling is shown in Fig. 3. The curves on the figures correspond to temperature profiles at time points equal to 0.1τ, τ and 4τ. The last one was defined above as the transient time. The highest curve in all figures corresponds to the steady-state temperature distribution. The voltage was chosen so as to provide an approximately equal (about 30°C) temperature increase in all instances. It can be seen from Fig. 3A that the temperature profile evolves by remaining almost uniform in the case of lack of forced cooling. It takes approximately 30 s to attain the steady state. The case of air cooling (Fig. 3B) is characterized by shorter transient times in comparison with the lack of forced cooling and greater temperature gradients of the buffer temperature. The electric field providing a temperature increase of 30°C is 190 V/cm, which is considerably greater than the 90 V/cm reported in Fig. 3A. With liquid cooling (Fig. 3C) the voltage is increased up to 360 V/cm and the transient time decreases to 1.36 s. However, the temperature gradient in the buffer becomes more pronounced and assumes a quasi-parabolic profile in the lumen of the capillary.

Results illustrating the influence of cooling and the type of capillary are presented in Table II. We took the temperature increase of 30°C as a reference point and calculated the transient times and electric fields necessary to produce such an elevation of temperature for all combinations of capillary types and cooling conditions. When comparing the values for thin and intermediate capillaries in Table II one might conclude that a threefold increase in capillary inner diameter does not lead to considerable changes in transient times for all modes of cooling. However, an increase in transient times of about 20% occurs. The transition to a thick capillary shows a considerable increase in transient times (by a factor of *ca.* 4). It can be seen from Table II that the transient process should be taken into account when performing separations in the absence of cooling for all type of capillaries, especially for thick ones. With

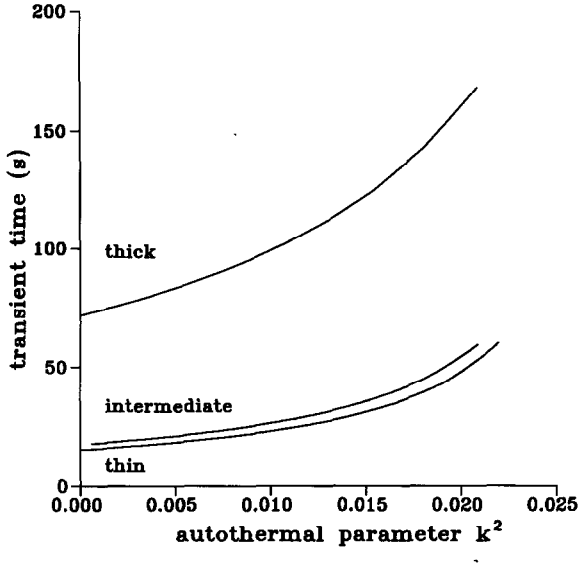

Fig. 4. Dependence of the transient time (in seconds) on the autothermal parameter (k^2) in the case of lack of forced cooling. Thin = capillary of 50 μm I.D. and 363 μm O.D.; intermediate = 150 μm I.D. and 363 μm O.D.; thick = 530 μm I.D. and 700 μm O.D. Note how the thin and intermediate capillaries behave similarly, whereas a large deviation is seen with the thick capillary.

air cooling these effects are pronounced only for thick capillaries and with liquid cooling their influence on separation appears to be negligible.

As the lack of cooling corresponds to longer transient times than other modes of cooling, we present dependences of the transient time on the autothermal parameter, eqn. 7c. This parameter is responsible for the autothermal runaway, as is evident from eqns. 9a and b. Fig. 4 shows these dependences for three types of capillaries and illustrates the progressive increase in transient time with higher values of the autothermal parameter (*i.e.*, increasing power generation).

The dependences of the transient time for the three capillary types on the heat-transfer coefficient are shown in Fig. 5, which generalizes our previous considerations to diverse kinds of coolants, cooling systems, etc. The electric field for each curve was adjusted so as to match the temperature for each capillary type at a given value of heat-transfer coefficient. Fig. 5 shows the importance of the capillary outer diameter on the transient process. It

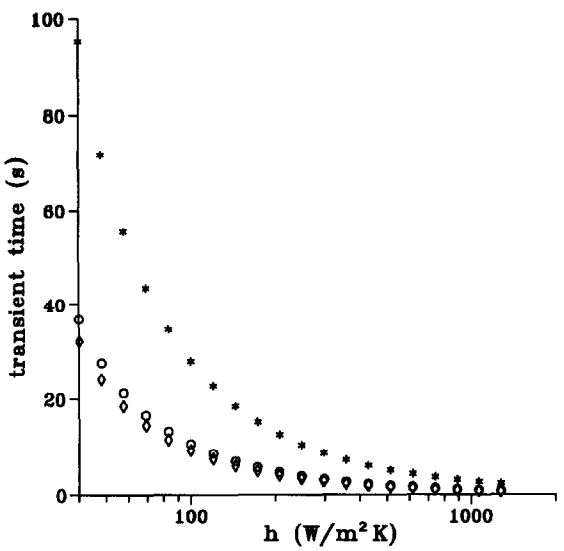

Fig. 5. Dependence of the transient time for three capillary types on the coefficient of heat transfer [h (W/m^2 · K)]. As in Fig. 4, note the very similar behaviour of the thin (◇) and intermediate (○) capillaries and the strong divergence of the thick capillary (✳). Note that, for any given value of the heat-transfer coefficient, the temperature on each of the three curves will coincide (this is obtained by adjusting the electric field strength in each type of capillary). E: ✳ (thick capillary), 32 V/cm; ○ (intermediate capillary), 110 V/cm; ◇ (thin capillary), 260 V/cm.

can be used for choosing a capillary type for a given cooling system or for the determination of the parameters of a cooling system.

CONCLUSIONS

Some practical guidelines can be derived from our simulations of thermal transients as follows.

In systems lacking forced cooling, the best operating mode would be at constant current, as this is the system generating the lowest temperature increase due to Joule heating.

In uncooled capillaries, the highest theoretical plate number will be obtained with the narrowest bore (*e.g.*, 20 μm I.D.), as this will correspond to the minimum radial temperature excursion.

As the thermal transients can last as long as >2 min, they will probably not be relevant in long-duration separations (typical of protein and nucleic acid analyses in gel media) but they might affect short-duration runs, *e.g.*, separations occurring in just a few minutes.

In very large-bore capillaries (*ca.* 500 μm I.D.), if there is a large temperature difference between the axis and the periphery, two phenomena will contribute to zone broadening (decrease in theoretical plate number): (a) radial viscosity gradients, allowing for faster migration of ions at the centre of the lumen (this will automatically generate conductivity differences) and (b) radial pH gradients, due to pK variations of the buffering ions in the background electrolyte (*e.g.*, the dpK/dT value for Tris is 0.03) [12], with a concomitant modulation of the mobility of the analyte ions, especially at background electrolyte pH values close to the pK values of the analytes.

Our results can be generalized to other types of separations, *e.g.*, isoelectric focusing in thin gel slabs (500 μm thickness). As these gels are cooled only on one side (see Fig. 3.13 in ref. 13), it is clear that temperature gradients will be pronounced (with generation of a radial pH gradient, in addition to the longitudinal pH gradient established between the anode and cathode). This definitely calls for gels of much decreased thickness (*e.g.*, 50–100 μm, simulation in progress).

ACKNOWLEDGEMENTS

M.S.B. thanks the European Space Agency (ESA)

for a fellowship enabling him to carry out this work at the University of Milan. P.G.R. thanks ESA, ASI (Agenzia Spaziale Italiana) and Progetto Finalizzato Chimica Fine II (CNR, Rome) for funding these studies.

REFERENCES

1 R. J. Nelson, A. Paulus, A. S. Cohen, A. Guttman and B. L. Karger, *J. Chromatogr.*, 480 (1989) 111–127.
2 W. A. Gobie and C. F. Ivory, *J. Chromatogr.*, 516 (1990) 191–200.
3 H. J. Issaq, I. Z. Atamna, G. M. Muschik and G. M. Janni, *Chromatographia*, 32 (1991) 155–161.
4 E. Grushka, R. M. McCormick and J. J. Kirkland, *Anal. Chem.*, 61 (1989) 241–246.
5 A. E. Jones and E. Grushka, *J. Chromatogr.*, 466 (1989) 219–225.
6 A. Vinther and H. Søberg, *J. Chromatogr.*, 559 (1991) 3–26.
7 G. O. Roberts, P. H. Rhodes and R. S. Snyder, *J. Chromatogr.*, 480 (1989) 37–67.
8 S. Terabe, *Trends Anal. Chem.*, 8 (1989) 129–134.
9 H. S. Carslaw and J. C. Jaeger, *Conduction of Heat in Solids*, Clarendon Press, Oxford, 2nd ed., 1959.
10 S. Kakaç, R. K. Shah and W. Aung (Editors), *Handbook of Single-Phase Conductive Heat Transfer*, Wiley, New York, 1987.
11 M. S. Bello and P. G. Righetti, *J. Chromatogr.*, 606 (1992) 95–102.
12 P. Lundahl and S. Hjertén, *Ann. N. Y. Acad. Sci.*, 209 (1973) 94–111.
13 P. G. Righetti, *Isoelectric Focusing: Theory Methodology and Applications*, Elsevier, Amsterdam, 1983.